Supporting Information

Template synthesis of 2D carbon nanosheets: Improving energy density of supercapacitors by dual redox additives of anthraquinone-2-sulfonic acid sodium and KI

Xiao Na Sun, Dong Xu, Wei Hu, and Xiang Ying Chen*

*School of Chemistry & Chemical Engineering, Anhui Key Laboratory of Controllable Chemistry Reaction & Material Chemical Engineering, Hefei University of Technology, Hefei, Anhui 230009, P. R. China. * The corresponding author. E-mail: cxyhfut@gmail.com.*

Structure characterization

The visualized morphology of the carbon sample was characterized by field emission scanning electron microscopy (FESEM; Hitachi S-4800, operated at a voltage of 10 kV). High-resolution transmission electron microscope (HRTEM) images and selected area electron diffraction (SAED) pattern were performed with a JEM-2100F unit. X-ray diffraction (XRD) pattern was obtained on a Rigaku D/MAX2500V with Cu Kα radiation. Raman spectrum was recorded at ambient temperature on a Spex 1403 Raman spectrometer with an argon-ion laser at an excitation wavelength of 514.5 nm. The specific surface area and pore structure of the carbon sample were determined by N_2 adsorption-desorption isotherms at 77 K (Quantachrome Autosorb-iQ). The specific surface area was calculated by the BET (Brunauer-Emmett-Teller) method. Pore size distribution were calculated by using a slit/cylindrical nonlocal density functional theory (NLDFT) model.

The electrochemical measurements conducted in a three-electrode system

A three electrode system was executed in the prepared electrolytes with a counter electrode of platinum foil (6 cm^2) and a reference electrode of saturated calomel electrode (SCE), and the three electrode experimental setup taking a 1 mol L^{-1} KNO_3 aqueous solution as electrolyte was used in cyclic voltammetry (*abbr*. CV) and galvanostatic charge-discharge (*abbr*. GCD) and electrochemical impedance spectroscopy (*abbr*. EIS) techniques measurements on an electrochemical working station (CHI660D, ChenHua Instruments Co. Ltd., Shanghai). The EIS measurements were carried out in the frequency range from 100 kHz to 0.01 Hz at open circuit potential with an ac perturbation of 5 mV.

For non-linear GCD plots, specific capacitances derived from them can be calculated from the equation:

$$C = \frac{I\mathrm{d}t}{m\mathrm{d}U} = 2\frac{I/m\int_{t_i}^{t_f} U\mathrm{d}t}{U^2\Big|_{U_i}^{U_f}} \qquad (1)$$

where C (F g^{-1}) is the specific capacitance; I (A) is the discharge current; t (s) is the

discharge time; $\int U\mathrm{d}t$ is the integral current area, where U (V) is the potential with initial and final values of U_i and U_f, respectively; and m (g) is the mass of active materials loaded in working electrode.

The preparation of electrode and electrochemical measurements conducted in a two-electrode system

In a two-electrode cell, a glassy paper separator was sandwiched between two electrodes, and each electrode contains a mixture of 80 wt% the carbon sample, 15 wt% graphite and 5 wt% polytetrafluoroethylene (PTFE) binder. Graphene paper serves as the current collector.

Specific energy density (E) and specific power density (P) derived from galvanostatic tests can be calculated from the equations:

$$E = \frac{I\int V\,\mathrm{d}t}{M} \tag{2}$$

$$P = \frac{E}{t} \tag{3}$$

E is the energy density; I is the current and M is the total active mass of both electrodes; $\int V\mathrm{d}t$ is the galvanostatic discharge current area; P is the power density and t is the discharge time.

For non-linear GCD plots, energy efficiency (η_E) was calculated using the equation:

$$\eta_E = \frac{\Delta t_{\mathrm{int}/d}}{\Delta t_{\mathrm{int}/c}} \tag{4}$$

where $\Delta t_{int/\mathrm{c}}$ and $\Delta t_{int/\mathrm{d}}$ are the integral charging and discharging time, respectively.

Properties	
Formula	Mg
Formula Weight:	24.31 g/mol
Assay	99.98% trace metals basis
Form	Shavings
Particle size	4-30 mesh
Melting point	648 °C (lit.)
Density	1.74 g/mL at 25 °C(lit.)
Vapor pressure	1 mmHg (621 °C)
TEST	**Specification**
Appearance (Color)	Conforms to Requirements
Particle Size Distribution	+4,+10,+30 mesh
ICP Major Analysis	Confirms Magnesium Component
Trace Metal Analysis	≤ 300.0 ppm
X-Ray Diffraction	Conforms to Standard Pattern
Purity	Meets Requirements

Table S1: The information of magnesium powder

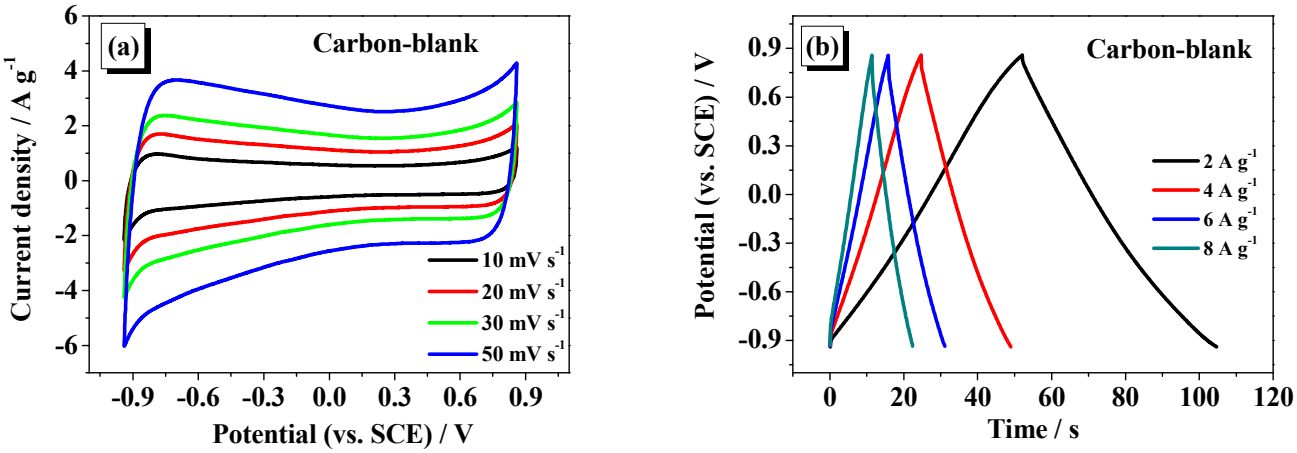

Figure S1. The **Carbon-blank** sample when measured in a three-electrode system: (a) CV curves at different scan rates; (b) GCD curves at different current densities.

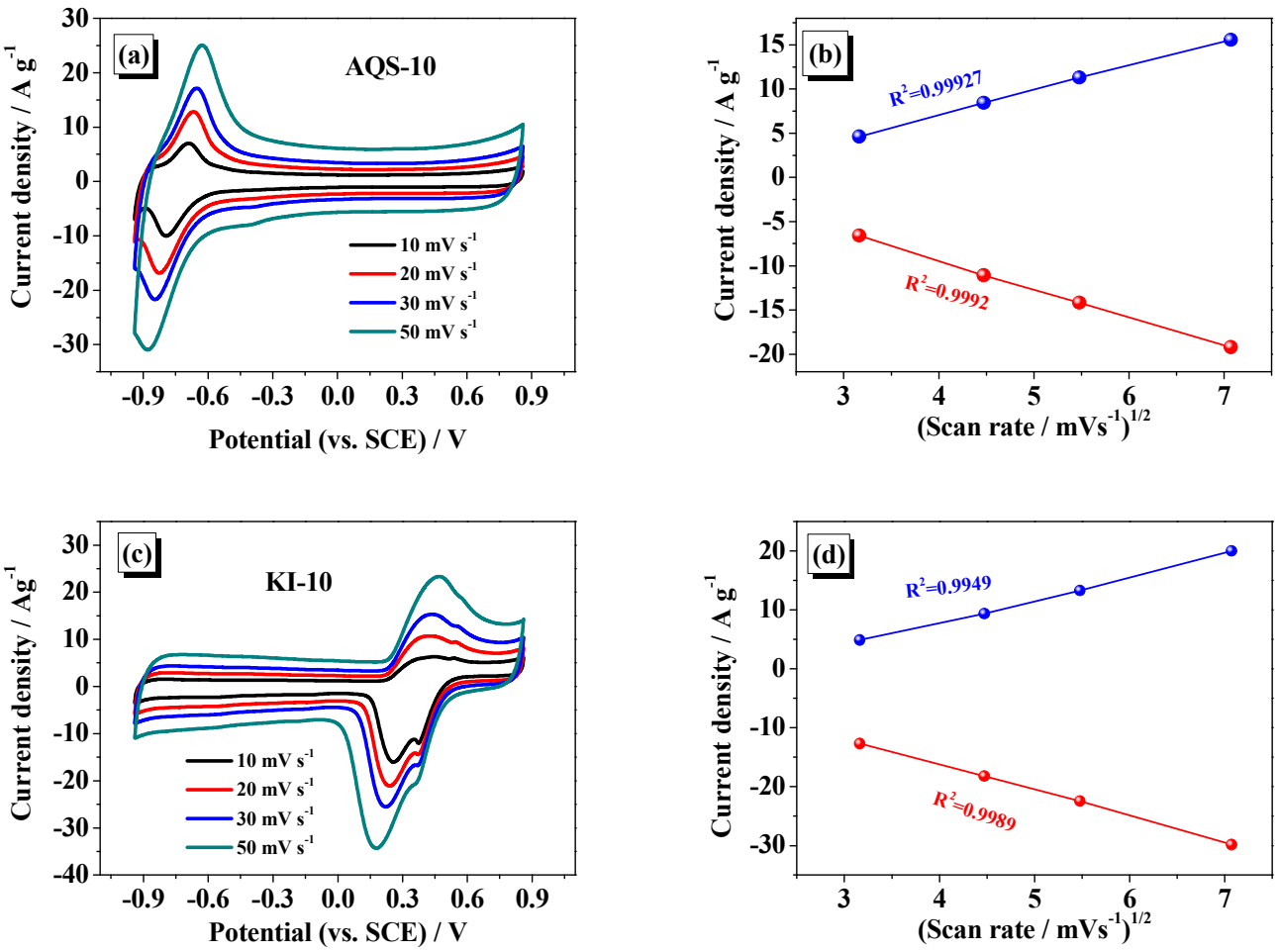

Figure S2. The **AQS-10**, **KI-10** samples measured in a three-electrode system: (a,c) The CV curves at different scan rates; (c,d) The linear relationship between current densities and scan rates.

In order to further evaluate the stability of supercapacitors more accurately. The floating test was also applied to the supercapacitors.[1,2] To put it simply, the **Carbon-blank** and **AQS:KI-1:1** samples were performed between 0 V and 1.8V utilizing a constant current density of 1 A g^{-1}. Every 4h of adding, five GCD cycles were applied. Then, the specific capacitance was calculated from the first and fifth discharging time, respectively. These sequences were repeated 50 times, a total floating time of 200h. And the results are shown below:

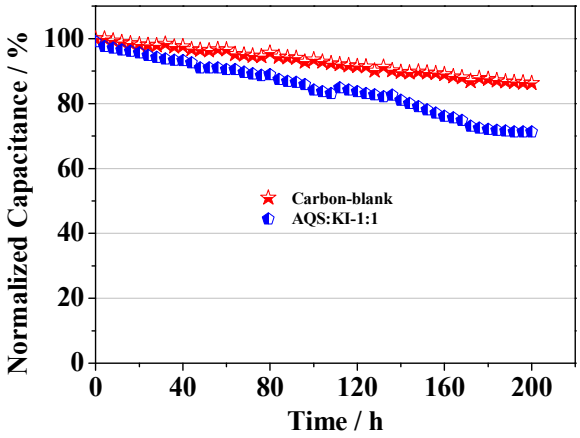

Figure S3. The floating test of the **Carbon-blank** and **AQS:KI-1:1** samples: The specific capacitance *vs* the floating time.

The results indicate that the AQS:KI-1:1 sample still has a good stability. In addition, many researchers have also reported the redox active electrolyte is a simple but effective approach to improve the capacitive performance of supercapacitors and also exhibits the stable performance.[3-5]

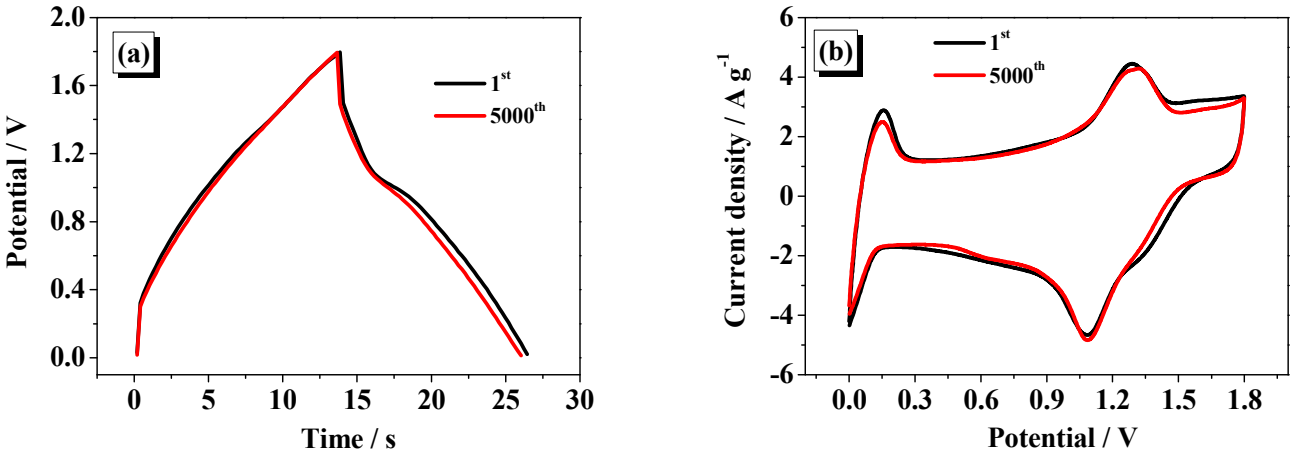

Figure S4. The **AQS:KI-1:1** sample measured in a two-electrode system: (a) The CV curves before/after 10000 cycles at 10 A g^{-1}; (b) The GCD curves before/after 10000 cycles measured at 20 mV s^{-1}.

In order to make clear the relation of the capacity and the frequency of supercapacitor, the picture of the imaginary part (C") of the capacitance vs. the frequency has been shown according to following equation:

$$C''(\omega) = \frac{Z'(\omega)}{\omega |Z(\omega)|^2} \tag{5}$$

Where Z' is the real parts of the impedance spectrum and |Z(ω)| is the impedance modulus.[6] The C" value corresponds to energy dissipation of the capacitor by an irreversible faradaic charge transfer process, which can lead to the hysteresis of the electrochemical processes.[7-9]

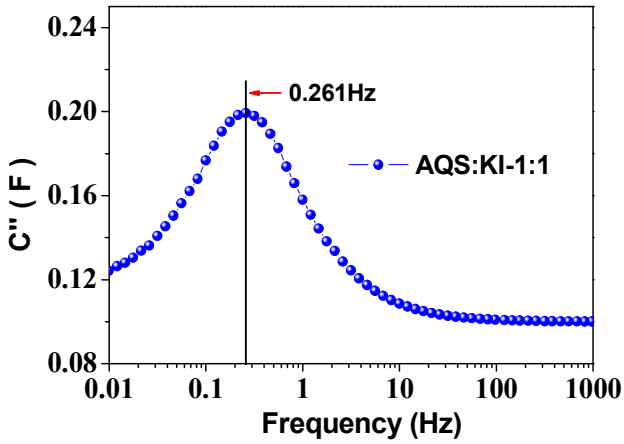

Figure S5. Imaginary part of capacitance (C") vs. frequency dependences

According to the results of the above picture, the C" achieve a maximum at a particular frequency of 0.261 Hz. And this frequency is called knee-frequency (f_k). On the other hand, the f_k determines the dielectric relaxation relaxation time (τ), which is an important parameter for the supercapacitors and can be calculated by the following equation:[10]

$$\tau = \frac{1}{f_k} \tag{6}$$

It is generally known that the smaller value indicates a smaller time for the supercapacitors to reach the half of the low frequency capacitance, indicating the

better properties of the system.[11] The relaxation relaxation time of the AQS:KI-1:1 sample was calculated as 3.83s. And this value displays that the 50% of the system capacitance can be reached within a short time of 3.83s at a low frequency.

References

(1) Weingarth, D.; Foelske-Schmitz, A.; Kötz, R. Cycle Versus Voltage Hold – Which Is the Better Stability Test for Electrochemical Double Layer Capacitors? *J. Power Sources* **2013**, *225*, 84–88. DOI:10.1016/j.jpowsour.2012.10.019

(2) Bello, A.; Barzegar, F.; Madito, M. J.; Momodu, D. Y.; Khaleed, A. A.; Masikhwa, T. M.; Dangbegnon, J. K.; Manyala, N. Stability Studies of Polypyrole-Derived Carbon based Symmetric Supercapacitor via Potentiostatic Floating Test. *Electrochim Acta* **2016**, *213*, 107–114. DOI: 10.1016/j.electacta.2016.06.151

(3) Mai, L. Q.; Khan, A. M.; Tian, X.; Hercule, K. M.; Zhao, Y. L.; Lin, X.; Xu, X. Synergistic Interaction between Redox-active Electrolyte and Binder-Free Functionalized Carbon for Ultrahigh Supercapacitor Performance. *Nat. Commun.* **2013**, *4*, 2923. DOI: 10.1038/ncomms3923

(4) Roldán, S.; Blanco, C.; Granda, M.; Menéndez, R.; Santamaría, R. Towards a Further Gneration of High-Energy Carbon-Based Capacitors by Using Redox-Active Electrolytes. *Angew. Chem. Int. Ed.* **2011**, *50*, 1699–1701. DOI: 10.1002/anie.201006811

(5) Fan, L. Q.; Zhong, J.; Wu, J. H.; Lin, J. M.; Huang, Y. F. Improving the Energy Density of Quasi-Solid-State Electric Double-Layer Capacitors by Introducing Redox Additives into Gel Polymer Electrolytes. *J. Mater. Chem. A* **2014**, *2*, 9011–9014. DOI:10.1039/c4ta01408a

(6) Taberna, P. L.; Simon, P.; Fauvarque, J. F. Electrochemical Characteristics and Impedance Spectroscopy Studies of Carbon-Carbon Supercapacitors. *J. Electrochem. Soc.* **2003**,*150*, 292–300. DOI: 10.1149/1.1543948

(7) Thomberg, T.; Jänes, A.; Lust, E. Energy and Power Performance of Vanadium Carbide Derived Carbon Electrode Materials for Supercapacitors. *J. Electroanal. Chem.* **2009**, *630*, 55–62. DOI: 10.1016/j.jelechem.2009.02.015

(8) Chen, K. F.; Liu, F.; Xue, D. F.; Komarneni, S. Carbon with Ultrahigh Capacitance When Grapheme Paper Meets $K_3Fe(CN)_6$. *Nanoscale* **2015**, *7*, 432–439. DOI:10.1039/c4nr05919k

(9) Jänes, A.; Lust, E. Use of Organic Esters as Co-Solvents for Electrical Double Layercapacitors with Low Temperature Performance. *J. Electroanal. Chem.* **2006**, *588*, 285–295. DOI: 10.1016/j.jelechem.2006.01.003

(10) Yu, H. J.; Fan, L. Q.; Wu, J. H.; Lin, Y. Z.; Huang, M. L.; Lin, J. M.; Lan, Z. Redox-Active Alkaline Electrolyte for Carbon-based Supercapacitor with Pseudocapacitive Performance and Excellent Cyclability. *RSC Adv.* **2012**, *2*, 6736–6740. DOI: 10.1039/c2ra20503c

(11) Yu, H. J.; Tang, Q. W.; Wu, J. H.; Lin, Y. Z.; Fan, L. Q.; Huang, M. L.; Lin, J. M.; Li, Y.; Yu, F. D. Using Eggshell Membrane as a Separator in Supercapacitor. *J. Power Sources* **2012**, *206*, 463–468. DOI: 10.1016/j.jpowsour.2012.01.116